

Supplementary materials for:

c

Panzhu Qin¹, Li Yao^{1,3}, Jianguo Xu^{1,*}, Guodong Liu^{2,3}, Wei Chen^{1,2,*}

¹ Engineering Research Center of Bioprocess, MOE, School of Food and Biological Engineering, Hefei University of Technology, Hefei, 230009, China

² Research Center for Biomedical and Health Science, School of Life and Health, Anhui Science & Technology University, Fengyang, 233100, China

³ Department of Chemistry and Biochemistry, North Dakota State University, Fargo, North Dakota, 58105, US

* Correspondence should be addressed to. Email: jgxu0816@163.com; chenweishnu@163.com

Table of contents:

- **Experimental section**
- **Table S1.** Oligonucleotides used in the current study
- **Table S2.** Comparison of different sensing protocols for nucleic acids detection
- **Figure S1.** Gel electrophoresis characterization of the dual-DNA machine
- **Figure S2.** Optimization of experimental conditions
- **Figure S3.** Real human serum samples screening
- **Figure S4.** Real cell samples screening

Experimental section

Materials and reagents

The T4 DNA ligase (5 U/ μ L) and Klenow fragment polymerase (3'-5' exo-) (5 U/ μ L) were purchased from Invitrogen, Thermo Fisher Scientific, Inc., (Shanghai, China), while the restriction endonuclease Nb.BbvCI (10 U/ μ L) was from New England Biolabs (Beijing, China). The SYBR Green I (20 μ g/ μ L) was obtained from Xiamen Biovision Biotech Co., Ltd (Xiamen, China). The deoxynucleotide triphosphates (dNTPs) were supplied by Sangon Biotechnology Co., Ltd (Shanghai, China). Other chemicals were of analytical grade and used without further purification. Ultrapure water obtained from a Millipore water purification system (18 M Ω cm⁻¹ resistivity) was used throughout the experiments. All oligonucleotide sequences (seen in **Table S1**) (dNTPs) were obtained from Sangon Biotechnology Co., Ltd (Shanghai, China) and dissolved with TE buffer (10 mM Tris-HCl, 1 mM EDTA, pH 8.0) to prepare the stock solution (10 μ M).

Fluorescence measurements

The fluorescence measurements were carried out at room temperature (RT) using a F97 Pro fluorescence spectrophotometer (Shanghai Precision Instrument Co., Ltd.). The fluorescence emission spectra in the range from 505 to 700 nm were collected in steps of 1 nm with an excitation at 490 nm. The excitation and emission slit widths were set at 10 nm. For biosensing, the fluorescence intensity at 520 nm in the absence and presence of target miRNA-21 was adopted for the assay performance evaluation.

Gel electrophoresis analysis

A droplet of 100× SYBR green I-stained samples (10 μL) with different components were loaded into electrophoretic lanes of a freshly prepared 12% native polyacrylamide gel electrophoresis (native-PAGE). The DNA analysis was performed in 1× TBE buffer at a constant potential of 80 V for 90 min, and the resultant gels were directly exposed to the UV light and photographed on a gel image system.

Procedure of dual-DNA machine-based miRNA-21 signaling

Prior to the assay, the hairpin-structured PHP was incubated at 95 °C for 2 min and then slowly cooled to room temperature over 30 min to make the probe perfectly fold into a hairpin structure. To carry out the dual-DNA machine for miRNA-21 analysis, the reaction mixture containing 1 μL of 10 μM PP, 1 μL of miRNA-21 at a fixed concentration, 1 μL of 10× ligase buffer, and 6 μL of double-distilled water (ddH₂O) was firstly denatured at 90 °C for 2 min. After slowly cooled down to room temperature about 10 min, 1 μL of T4 DNA ligase (5 U/μL) was injected and incubated at 16 °C for 30 min to implement the ligation reaction. Subsequently, 2 μL of 10× NEBuffer 2, 0.6 μL of Klenow fragment (3'-5' exo-) (5 U/μL), 0.5 μL of Nb.BbvCI (10 U/μL), 2 μL of 25 mM dNTPs, 2 μL of 10 μM PHP, and 2.9 μL ddH₂O were successively added into the above solution and incubated at 37 °C for 2.5 h. Finally, the reaction mixture was terminated by ice-bath and diluted with 10 mM PB (pH 7.0) for fluorescence recording.

Procedure of single-DNA machine-based miRNA-21 signaling

Given the single-DNA machine was conducted by the probe couples of PP/PHP* for RCA-CDM and PP*/PHP for CSDA-BDM, respectively, its operation was very similar as that of dual-DNA machine by only replacing the probe of PHP as PHP* for the former

DNA machine or replacing the probe of PP as PP* for the latter DNA machine. Other procedures were identically performed.

Real sample detection

For human serum samples (kindly provided by Liaocheng People's Hospital), they were pre-treated according to reported literature with minor modification.¹ Briefly, each of the serum samples was firstly diluted 5 times with PBS. Followed by heating at 95 °C for 5 min, the solution was immediately cooled on ice over 5 min and then freeze-centrifuged at 17000 g for 15 min to collect the supernatant. For cell samples, the human cervical cancer cell line of Hela was cultured in the Dulbecco's modified Eagle's medium (DMEM, high glucose) supplemented with 10% fetal bovine serum (FBS), 100 units/mL penicillin, and 100 mg/mL streptomycin. After grown as adherent monolayer in a humidified atmosphere containing 5% CO₂ at 37 °C, the cells were collected and finally extracted to collect the total RNA by Trizol-reagent in terms of indicated manufacturer instructor. After the pretreatments, both the serum samples and cell samples were identically measured in accordance with the abovementioned experimental procedures.

Table S1. Oligonucleotides used in the current study

Note	Sequence (5'-3')
Padlock probe (PP)	5'-P-CTGATAAGCTATACGCGTACTTCAACAACAAC <u>AACAACCCTCAGCTCAACATCAGT</u> -3'
Palindromic hairpin probe (PHP)	5'-DABCYL- <u>tacgctacttcAACAACAACAACAAC</u> CCTCAGC gaagtacgct(FAM)a-3'
Padlock probe* (PP*)	5'-P-CTGATAAGCTATACGCGTACTTCAACAACAAC <u>AACAACCAACAAC</u> TCAACATCAGT-3
Palindromic hairpin probe* (PHP*)	5'-DABCYL- <u>aaggtcccttcAACAACAACAACAAC</u> CCTCAGC gaaggaacc(FAM)t-3'
MiRNA-21	5'-UAGCUUAUCAGACUGAUGUUGA-3'
Mismatched 1 (M1)	5'-UAGCU <u>A</u> AUCAGACUGAUGUUGA-3'
Mismatched 2 (M2)	5'-UAGCUUAUCA <u>C</u> ACUGA <u>A</u> GUUGA-3'
Mismatched 3 (M3)	5'-UAGCU <u>A</u> AUCA <u>C</u> ACUGA <u>A</u> GUUGA-3'
MiRNA-10b	5'-UACCCUGUAGAACCGAAUUUGUG-3'
Let-7d	5'-AGAGGUAGUAGGUUGCAUAGUU-3'
MiRNA-141	5'-U AACACUGUCUGGUAAAGAUGG-3'
MiRNA-200b	5'-UAAUACUGCCUGGUAAUGAUGA-3'

For PP and PHP, the underlined sequence is identical designed and the bold fragment is the half cleavage site of Nb.BbvCI restriction endonuclease. The red-colored and green-colored bases in phosphorylated PP indicate the complementary regions of miRNA-21. The shadowed region in PHP denotes the palindromic sequence, and the lowercase letters help PHP fold into a hairpin-structured conformation, forcing the two labelled moieties of FAM and DABCYL closed to each other. The PP* and PHP* are similarly designed as PP and PHP but without the half cleavage site of Nb.BbvCI restriction endonuclease and palindromic sequence, respectively. NT1 and NT2 are the generated products from RCA-CDM and CSDA-BDM, respectively. M1, M2, and M3 are the target miRNA-21 analogue with one, two, and three bases mismatch projected in box. MiRNA-10b, miRNA-141, miRNA-200b, and let-7d are non-target species.

Table S2. Comparison of different sensing protocols for nucleic acids detection

Signaling method	S/N	Linear range	Order of amplification magnitudes	Detection limit	Reference
Fluorescent assay	~ 5	5 pM~ 20 nM	4	5 pM	2
Fluorescent assay	~ 2	5 nM~ 1 μ M	3	10 pM	3
Fluorescent assay	~ 3	3 aM~ 0.3 pM	5	52.5 zM	4
Colorimetric assay	~ 7	10 pM~ 200 nM	4	20 pM	5
Colorimetric assay	~ 5	20 pM~ 1 nM	2	100 fM	6
Electrochemical assay	~ 10	100 pM~ 5 nM	2	58 pM	7
Photoelectrochemical assay	~ 2	50 pM~ 100 nM	4	21.3 pM	8
Electro-chemiluminescence assay	~ 2	1 fM~ 100 pM	5	0.28 fM	9
Fluorescent assay	~ 24	1 pM~ 50 nM	4	10 fM	Current study

Gel electrophoresis characterization of the dual-DNA machine

To further confirm the feasibility, gel electrophoresis was performed to prove the principle. It can be found in **Figure S1** that lane a and lane b are the mixture of PP, PHP, and ligase in the absence and presence of target miRNA-21, respectively. lane a only shown the blurry bands of designed PP (upper band) and PHP (lower band) because the poor inserting ability of SYBR Green I towards oligonucleotides with very weak secondary structure. When target miRNA-21 was further incubated, a new bright band with high molecular weight than PP appeared in lane c, indicating the successful hybridization of miRNA-21 with PP. After incubation them with Klenow polymerase, the control sample in lane c only exhibited the lanes of PP and PHP, while the target sample in lane d appeared a series of bands, in where the majority was blocked in the loading hole. It is mainly because the occurrence of polymerase promoted-RCA in the presence of miRNA-21. More interestingly, as can be seen in lane f, further addition of Nb.BbvCI into the components of sample d to carry out the dual-DNA machine caused the generation of multiple bands with lower molecular weights but strong brightness than lane d, and the bands of PHP and PP were totally exhausted. These new bands proved the effect of enzymatic cleavage, the generation of nicked triggers, and the unfolding of massive PHP. In sharp contrast, lane e was still identical as lane a and c, implying the dual-DNA machine was completely restrained without the stimulus of miRNA-21. The gel image results were consistent with the change tendency of fluorescence measurements (**Figure 1**), convincing the rational construction of dual-DNA machine.

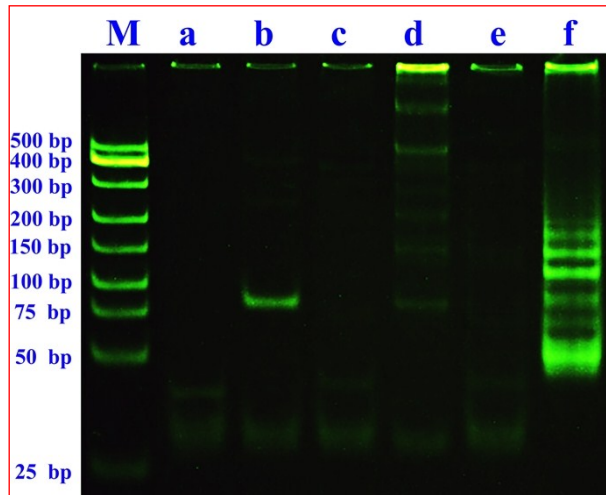


Figure S1. Gel evidence for the dual-DNA machine operation. Lane a, PP+PHP+Ligase; Lane b, PP+PHP+miRNA-21+Ligase; Lane c, PP+PHP+Ligase+Klenow; Lane d, PP+PHP+miRNA-21+Ligase+Klenow; Lane e, PP+PHP+Ligase+Klenow+Nb.BbvCI; Lane f, PP+PHP+miRNA-21+Ligase+Klenow+Nb.BbvCI.

Optimization of experimental conditions

In order to establish optimum conditions for miRNA-21 analysis, several essential parameters, such as the dosage of Klenow and Nb.BbvCI, and isothermal incubation time, were systematically examined. The obtained value of F/F_0 was adopted to evaluate the signal amplification efficiency, where F and F_0 were the peak fluorescence intensity in the presence and absence of target miRNA-21, respectively. As presented in **Figure S2A**, the F/F_0 increased obviously with increasing the dosage of Klenow from 1 to 3 U given more and more DNA machines would be activated for fluorescence reporting. However, the results shown that further increase of Klenow led to a decreased signal response, which was most likely due to the fact that the excessive usage of Klenow might induce a slightly improved background and inhibit the reaction of endonuclease. As the highest F/F_0 was achieved at 3 U Klenow, we thus chosen 3 U as the optimal dosage for operation of the DNA machine. Along a similar line, the change tendency of F/F_0 against the dosage of Nb. BbvCI in **Figure S2B** was identical to that of **Figure S2A**, suggesting the optimal Nb.BbvCI dosage was 5U. Actually, there is a dynamic equilibrium among the processes of DNA extension, chevage, and release to ensure the highly efficient operation of the proposed dual-DNA machine. Overuse of polymerase or endonuclease would make DNA extension or chevage occupy the dominant position, respectively, which was not helpful for the equilibrium construction and fluorescence output. Only under moderate conditions, the co-application of polymerase and endonuclease can generate a maximum synergistic effect for amplified miRNA signaling. **Figure S2C** revealed the results for isothermal incubation time

optimization. It can be seen that with the increasing of reaction time, the signal response elevated at a fast rate in the initial stage (0.5 to 2.5 h) because an increasing number of amplification events were involved, and then leveled off after 2.5 h in view of the reaction was adequately processed. Therefore, 2.5 h was adopted for the enzymatic reaction.

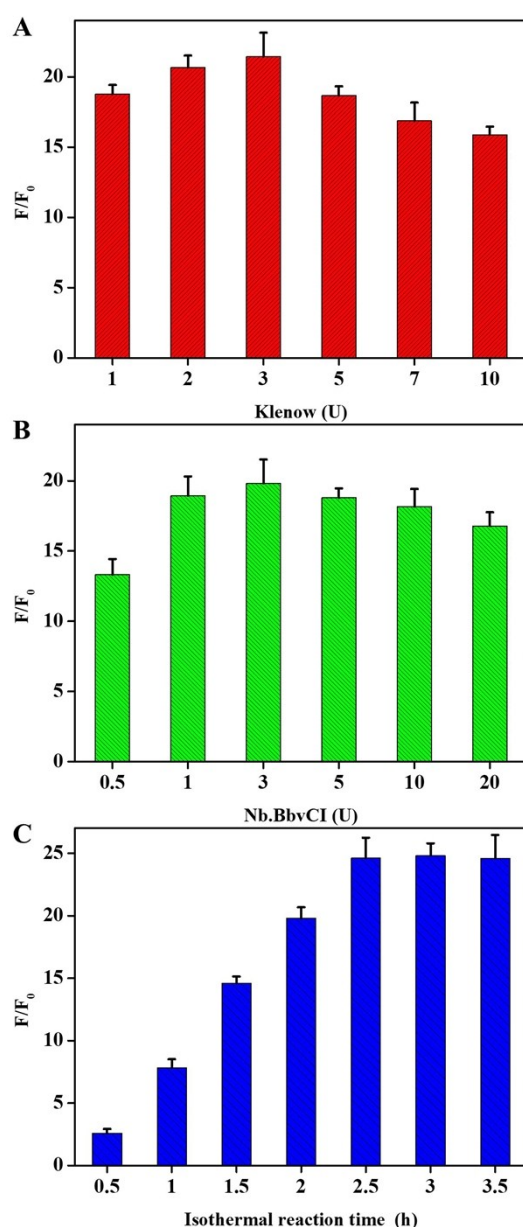


Figure S2. Effects of the polymerase dosage (A), endonuclease dosage (B), and isothermal incubation time (C) on the dual-DNA machine assay performance.

Real human serum samples screening

In order to evaluate the practical applicability of the dual-DNA machine, the clinical related human serum samples from four health donors and four patient donors were examined in **Figure S3**. We can notice that the responses of miRNA-21 in all patient donors (sample 5 to 8) are obviously stronger than those of health donors (sample 1 to 4), indicating that the expression level of miRNA-21 is upregulated in all serum samples of breast cancer patients. The results are well consistent with previous reported literatures, which have shown that the abnormal increased expression of miRNA-21 in serum can be adopted as a biomarker of breast cancer progression. Furthermore, given that the human serum is one of the most challenging media with a variety of proteins and other serious interferences, the results also reveal that the developed dual-DNA machine can be tolerant toward complex biological substrates for reliable and practical miRNA detection. Meanwhile, the detection of miRNA-21 from the cancer cell is also detailly given in Figure S3 and similar results can be observed.

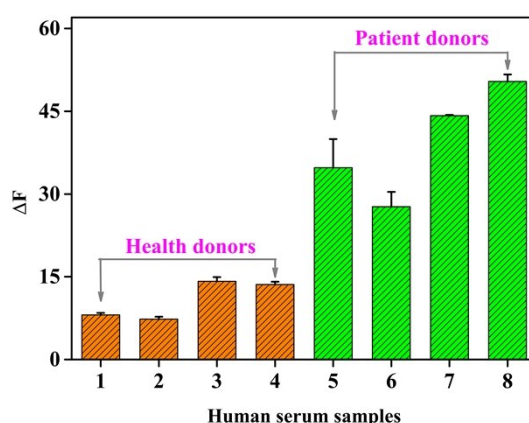


Figure S3. Expression profiles of miRNA-21 in real human serum samples. Sample 1 to 4 is collected from health donors, while sample 5 to 8 is collected from patient donors. The fluorescent intensity of ΔF is deduced as $F - F_0$, where F and F_0 represent the dual-DNA machine in the absence and presence of human serum samples,

respectively.

Real cell samples screening

To further confirm the practical application ability, the human cervical cancer cell line of HeLa was chosen as the real samples for miRNA-21 screening. It can be noticed in **Figure S4** a net increase of fluorescence intensity was achieved in the presence of extracted total RNA, and its response was increased with the increasing of cell numbers. The result is attributed to the fact that the miRNA-21 is expressed in HeLa cells, and its content level is positively correlated with the cell number, indicating the powerful applicability of the dual-DNA machine.

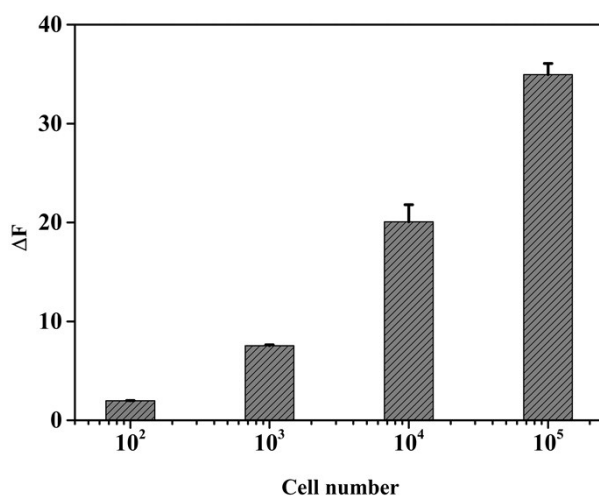


Figure S4. Extracted total RNA detection derived from 10^2 , 10^3 , 10^4 , and 10^5 HeLa cancer cells. Error bars represent at least three parallel repeats. The fluorescent intensity of ΔF is deduced as $F - F_0$, where F and F_0 represent the dual-DNA machine in the absence and presence of human serum samples, respectively.

Reference

1. Y. Li, L. Liang and C. Zhang, *Anal. Chem.*, 2013, 85, 11174-11179.
2. H. Xu, Y. Zhang, S. Zhang, M. Sun, W. Li, Y. Jiang and Z.-S. Wu, *Anal. Chim. Acta*, 2019, 1047, 172-178.
3. R. Liao, K. He, C. Chen, C. Cai and X. Chen, *Anal. Chem.*, 2016, 88, 4254-4258.
4. H. Dong, X. Meng, W. Dai, Y. Cao, H. Lu, S. Zhou and X. Zhang, *Anal. Chem.*, 2015, 87, 4334-4340.
5. Z. Shen, F. Li, Y. Jiang, C. Chen, H. Xu, C. Li, Z. Yang and Z. S. Wu, *Anal. Chem.*, 2018, 90, 3335-3340.
6. A. X. Zheng, J. Li, J. R. Wang, X. R. Song, G. N. Chen and H. H. Yang, *Chem. Commun.*, 2012, 48, 3112-3114.
7. Z. F. Gao, Y. Ling, L. Lu, N. Y. Chen, H. Q. Luo and N. B. Li, *Anal. Chem.*, 2014, 86, 2543-2548.
8. G. Wen, W. Dong, B. Liu, Z. Li and L. Fan, *Biosens. Bioelectron.*, 2018, 117, 91-96.
9. Z. Xu, Y. Chang, Y. Chai, H. Wang and R. Yuan, *Anal. Chem.*, 2019, 91, 4883-4888.